Mausam, (1981), **32**, 1, 1-10

551. 576.3 : 551. 515.1

Cloud top temperature structural changes during the life-cycle of Saurashtra cyclone (1978)

M. S. NARAYANAN and B. M. RAO

Meteorology Division, Space Applications Centre, Ahmedabad

(*Received 5 December 1979*)

ABSTRACT. Cloud Top Temperature (CTT) maps obtained for the first time in India from the NOAA-5 Very High Resolution Radiometer (VHRR) data recorded at Space Applications Centre, Ahmedabad have been analysed to study the intensity changes associated with the cyclonic storm of November 1978. A progressively southward movement of the deep convection cells in relation to the Central Dense Overcast (CDO) is observed from the intensifying to the final decay stage of the storm. The locations of these cells are shown to be an important factor associated with the cyclone intensity changes. The southward extension of westerlies is proposed as a possible cause of the southward shift of the deep convective cells within the CDO.

1. Introduction

The thermal infrared (IR) window channel (10-12 μ) radiance measurements from meteorological satellites are being now increasingly utilised for sea surface temperature (SST) and cloud top temperature/height (CTT/CTH) estimates. The estimation of these temperatures from IR data is based on the principle that thick clouds and sea surface radiate energy nearly like a blackbody. To date most of these measurements had been limited to estimates from the High Resolution Infrared Radiometer (HRIR) on Nimbus and scanning radiometer data from NOAA-3, 4 and 5 satellites. These sensors had a ground resolution of about 8 km.

At the Space Applications Centre (SAC), Ahmedabad, an S-band earth station was set up in April 1978 to receive the Very High Resolution Radiometer (VHRR) data from NOAA-5 satellite. The VHRR sensors have a resolution of 1 km at the sub-satellite point (ssp) providing data that could be used to estimate the surface and cloud top temperature parameters to about 1 deg. K accuracy.

In an earlier paper (Rao *et al.* 1980) we had discussed briefly our VHRR data reception system and the synoptic features during the different phases of the Saurashtra cyclone (1978) from the NOAA-5 VHRR imageries recorded at Ahmedabad between 6 and 12 November 1978.

In this paper we present the first results of the cloud top temperature maps of the Indian region from high-resolution sensor satellite data, recorded and processed in India. Bhaskara Rao and Saxena (1977) had reported earlier the first cloud top height results over the Indian region from the grid point radiance values obtained from NASA for the Nimbus-3 HRIR.

The cloud top height measurements are of considerable importance not only for understanding the lower to upper tropospheric energy exchanges (as in severe weather systems) but also find great operational use in aviation meteorology. Recently (Follansbee 1975 ; Scofeld and Oliver 1976 and Griffith *et al.* 1978) have suggested empirical methods to estimate rainfall amounts from sequential cloud top height measurements, which find great potential in hydrometeorological studies.

The results of data presented in this paper pertain to a cyclonic system which hit the Saurashtra coast on 11 November 1978. The structural and the cloud organisation changes that the cyclone underwent during the different stages (between 6 and 12 November 1978) of

development and decay are presented from the available data using the cloud top temperature maps. Our attempts were also to investigate suitable objective criteria for the intensity estimate of the cyclones from CTT measurements.

The details of VHRR data calibration, methodology of CTT mapping and other data processing algorithms developed by us are also presented.

2. Cloud top heights and intensity of storm

Latent Heat Release (LHR) associated with warm moist tropical air ascent in major cumulus towers of cyclones is the primary fuel for the storms (Dunn and Miller 1960) and its availability is indicated by the vigour of the convection within the cyclone which can be deduced from cloud top temperature measurements. Thus satellite measured equivalent blackbody temperatures (T_B) of cloud tops in tropical cyclones should contain useful information about storm intensity and expected changes of intensity. The theoretical numerical model of Rosenthal (1978) suggests that maximum convection precedes maximum surface winds by 1-3 days.

The areal distribution of T_B provides information showing the extent and strength of the convection which serve as indices of latent heat released and indicate the extent that the clouds of the storm are organised into patterns. The subsiding air motions can also be observed from the analysis of T_B maps when cloud tracers are available.

Dvorak (1975) and others have developed techniques to identify the present inensity of the tropical cyclone and to suggest future changes of the intensity from the satellite imageries. While these techniques need great skill and are in widespread use in the tropics worldwide, it still involves considerable subjectivity especially in the forecasting of storm intensity.

Gentry *et al.* (1978) advanced a hypothesis which says:

(*i*) The T_B of tropical cyclone cloud tops provide a measure of the convection and an index of the LHR for eventual conversion to kinetic energy.

(*ii*) The T_B areal distribution serves as an index of the organisation of the storms' convective activity, and

(*iii*) the lower the mean T_B of the cloud tops over a moderate sized area, the stronger and more persistent is the convection and the more likely that the maximum winds in the storm will increase with time.

TABLE 1

Date	Time (IST)	T No.
5 November 1978	15.47	3.0
6 November 1978	15.38	4.5
7 November 1978	15.30	5.5
8 November 1978	15.19	6.5
9 November 1978	16.51	5.0
10 November 1978	16.41	4.0
11 November 1978	16.31	3.0

Recently Dvorak and Wright (1978) and Erickson (1979) have also suggested objective *cum* subjective methods for estimating storm intensity on an operational basis.

We have analysed some data to apply these hypothesis to the VHRR data recorded at SAC and to relate the intensity estimates to the T_B. The IR data have been analysed to study cloud top temperatures for different days for the organised cyclone in the Central Dense Overcast (CDO) area to estimate:

(*i*) locations of active convection zones (penetrating/overshooting towers) and their areal extent,

(*ii*) their temperature/height,

(*iii*) sector-wise distribution, and

(*iv*) areas and extents of subsidence.

We have assumed that all the features that go to make up the final T-No. (intensity of cyclone) should be reflected in the convective and subsidence patterns and their areal distribution.

3. Data

For the analysis, we have used the digital data on CCT corresponding to the day-time passes on 6, 9, 10, 11 and 12 November 1978 of the NOAA-5 VHRR thermal IR band. The storm under investigation formed as a low in the Bay of Bengal on 3 November, crossed the Peninsula, intensifying to the cyclonic storm stage on 5 November, reaching its peak intensity on 8 November. After 10 November night it started getting disorganised and hit the Saurashtra coast on 11 November night. The track of the storm is shown in Fig. 1. The T-No. intensity estimate of the storm for the different days as supplied by the India Met. Dept. are given in Table 1.

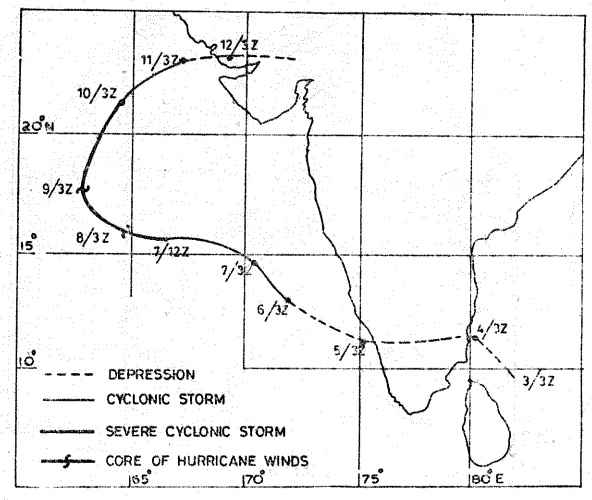

Fig. 1. Track of Saurashtra cyclone (November 1978)

Geometric correction

The NOAA-5 imagery has got geometric distortion beyond about 1000 km on either side of the subsatellite point. One could correct the picture for this distortion on computer (generating a new CCT for the imagery), for calculating distortion-free lengths and areas in the picture. However, we have tried a slightly less rigorous method by using a curve which shows the variation of the area of one pixel (one picture element of area nearly 1 km² at ssp) as a function of its distance from the ssp. The area of any portion of the imagery is transformed to correct areas using the curve knowing the distance of the area from the ssp track.

4. Calibration procedure

The calibration procedure consists essentially of establishing a relationship between IR grey levels (G) and corresponding raw temperatures (T), with the help of a set of 12 parameters, transmitted alongwith the VHRR data stream of each scan line.

Although the onboard black body temperature was found to be constant to better than 0.3 deg. C from scan line to scan line in the computations, it was observed that there was an appreciable line-to-line and short term variation in the other parameters. A fairly large ($\sim$5 deg. C) temperature difference for same values of G, particularly between the normally encountered grey levels (70 to 90) has been observed by us.

We have tried to eliminate the effects of the line-to-line noise by an averaging process. Groups of 100, 200 and 500 scan lines were selected for the averaging process. In comparison a 5 min satellite pass contains 2000 scan lines. The selection of scan lines was to a certain extent random, *viz.*, that of selecting every 5th line or 3rd line from the data tape of a particular pass.

From a study of the G *vs* T curve for a single scan line and for a set of 200 and 500 scan lines it can be seen that the maximum departure in the G *vs* T relation exists between the grey values 50 to 100, which is in the observation range. An entirely different set of 500 lines of the same pass was also used to generate a G *vs* T curve. These differed from the first set of 500 scan lines by not more than 0.5 deg. C at any grey level value. This was considered a fair enough accuracy at present, considering other limitations.

5. Method of analysis

Three different methods have been employed to study the organisation of cloud tops in the infrared imagery:

(*i*) Histogramming,

(*ii*) Computer printout, and

(*iii*) Enhancement techniques.

The first two yield quantitative information, while the third, prepared on the basis of the results of first two, is used mainly for visual interpretation of the processing.

5.1. *Histogramming*

Frequency distribution in the area of interest of each grey count in the picture is determined. From this, one knows the total temperature range of the surface and cloud tops and their relative population. The low and high level clouds can be distinguished from the relative higher and lower temperatures.

5.2. *Picture printout*

This is the most important part of the digital data processing from which quantitative estimates and fine structural details of cloud tops can be made. After knowing the frequency distributions, the digital 2-dimensional map of the cloud top temperature of the area is prepared, assigning different characters to each temperature grey level range. In general 6-8 groups of temperature range are selected, and each group assigned a character.

From practical considerations, grey values of a set of pixels and scan lines are averaged to assign a single character corresponding to the average grey level (or temperature).

This process yields a thematic map, from which locations of clouds, their temperature, and area can be measured. The so called *'hot towers'*, which are the main energy supplying regions to the cyclone are easily recognised from these maps and regions. Areas and regions of suppression of cloud growth and subsidence can also

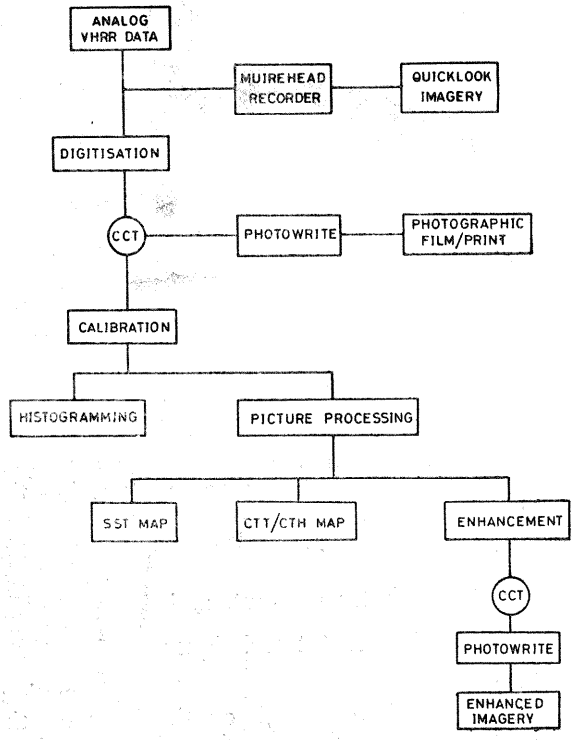

Fig. 2. Digital picture processing flow chart

be distinguished by their relatively higher temperatures. Sea surface areas can aso be distinguished.

5.3. *Enhancement technique*

This is but a slightly different and a photographic version of the picture printout. The different temperature groups chosen from the picture printout are suitably amended (in case it is felt desirable to reduce the number of groups). The grey values of pixels in original CCT are converted to suitably chosen new grey values and written on another CCT, which is then photo-written to get a photograph for visual inspection. It may be noted that there may not be any averaging of pixel grey level values as in picture printout, but individual pixel values are set to new grey values. However, to reduce the noise in the original data suitable averaging can be employed.

To improve the contrast between even small grey level differences, various step-grey level and non-linear enhancement curves have been employed by us. The result is that the normally available total dynamic range (0-255) itself gets multiplied to give an effective dynamic range that is a few times 256.

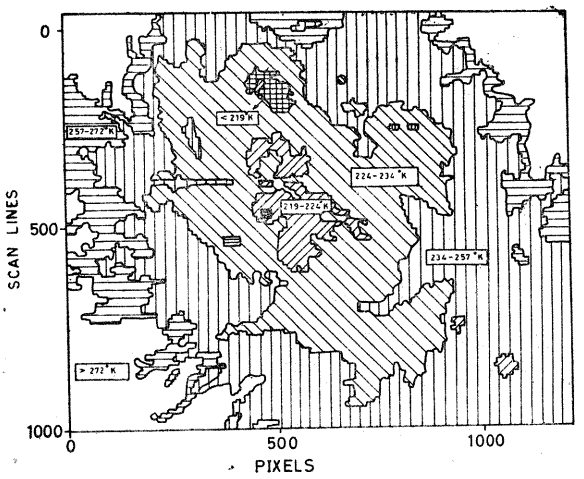

Fig. 3. Cloud top temperature map of 6 November 1978

This product, when obtained interactively on a TV screen assumes special importance to know areas of various levels of deep convection, subsidence, sea surface etc. Various enhancement curves can be employed each suiting to different requirements. These are under development by us.

5.4. *Flow diagram of computer processing*

In the flow diagram (Fig. 2) the processing methods from the time data acquired to the final product stage is detailed. All the processings have been implemented on IBM 360 system 44 on a batch processing mode and in modular form. The picture printout module has many versatalities many of which will find great applications in SST, CTT, cloud top height mapping, snow cover delineation, land-sea contrast, etc.

6. Results

The IR imageries of 6, 9, 10, 11 and 12 November that have been analysed are presented in Figs. 4 (a) to (e). The areas that have been processed are indicated by a grid.

The atmospheric attenuation due to the presence of water vapour has not been incorporated in these results, as the corrections due to these are important only upto about 4-5 km above the sea level. Our studies pertain to levels which are beyond about 6-7 km, hence these corrections are negligible.

Knowing the grey level limits of the imagery from the histogram the picture printout for 6 November in a modified form is presented in Fig. 3. As the computer print characters are not squares, the actual areas from the original printouts have been redrawn manually in a graph to appropriate scale.

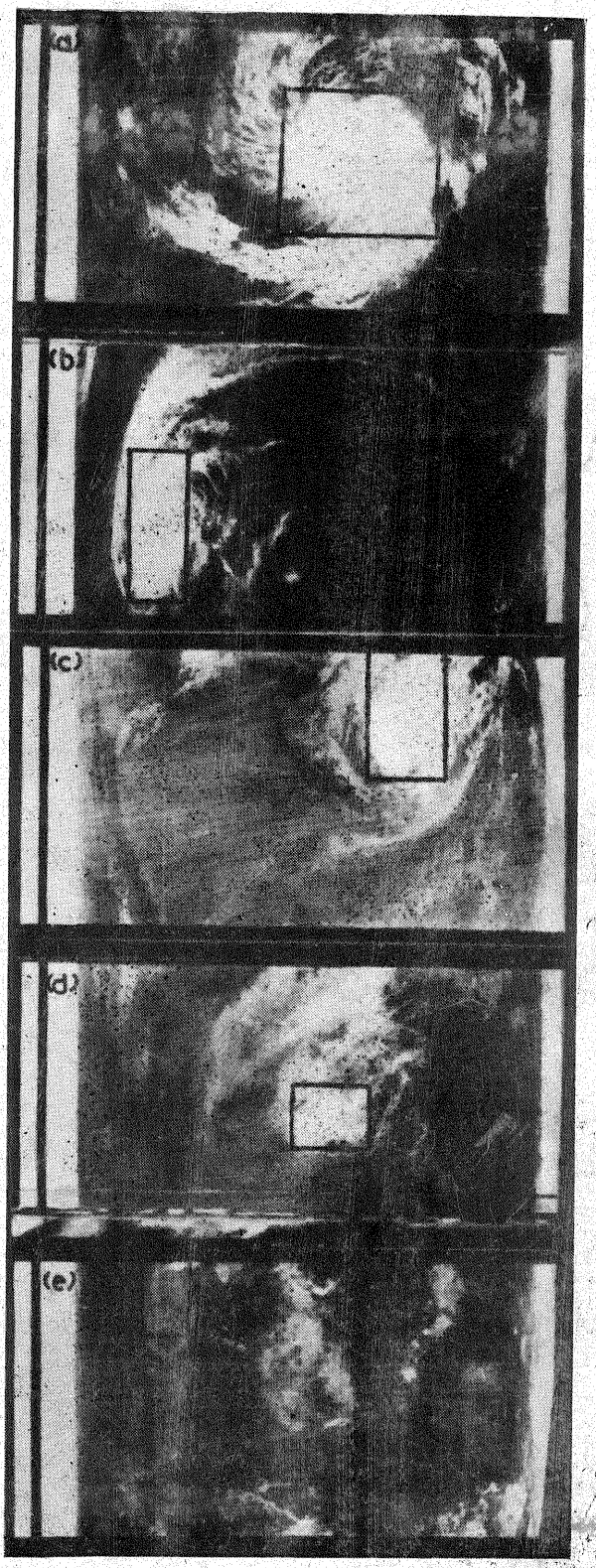

Fig. 4. Infrared imageries of Saurashtra cyclone

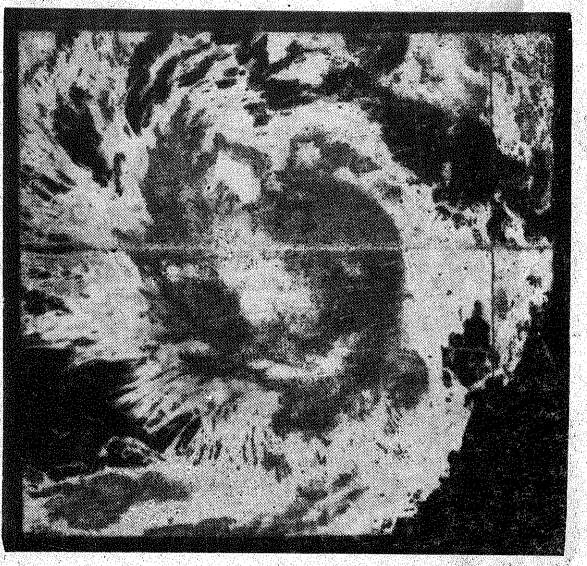

Fig. 5. Enhanced imagery of cyclone of 6 November 1978

In this picture, different classes of temperatures have been designated. The area occupied by each contour can be calculated from the help of the histogram table and the picture distortion curve. From the temperatures the Cloud Top Heights (CTH) can be calculated assuming a standard atmospheric lapse rate.

A step-*cum*-linear enhancement curve was applied to the input data of 6 November 1978. Linear portion was used to enhance the outer cloud features and the step portion for the inner features of the cloud. The result of this enhancement is shown in Fig. 5. Though some inherent noise of the original data has appeared a little magnified in the enhanced picture, it can be seen that the boundary of the different classes are more clearly defined. In fact the exercise involved in the enhancement technique for cloud height delineation for cyclones is in tuning the input and output grey ranges (the step portion of the enhancement curve) to get the sharpest contrast for various class boundaries.

Similar analysis were performed and maps prepared from the data of 9, 10, 11 and 12 November. Areas of cloud coverage, active convection, their number and sectorwise distribution, height of highest cloud etc were determined from the picture printout. In the picture printout maps of 9 and 10 November (Figs. 6 and 8) no modification for computer character distortion has been made. The areas of subsidence and inhibition of cloud growth are distinguishable only when the cloud tracers are present, and the interpretation in terms of subsidence is made when cloud top temperature is more than 270 deg. K and in the clear areas of sea. Such areas were also located.

To delineate cloud boundaries and areas of deep convection we have chosen two somewhat arbitrary criteria which are, however, based on some physical considerations.

A 255 deg. K temperature contour in the picture printout map was fixed to delineate cloud boundary. Griffith *et al.* (1978) from a simultaneous analysis of radar and geostationary imageries have observed that clouds below this temperature contribute nearly 90 per cent to the radar echoes of rains. The boundary for deep convective cells was delineated by the cloud top temperature contour of 235 deg. K (corresponding to clouds above about 10 km).

In the next subsections that follow, details of cloud top organisation for the five days of analysis is presented.

6.1. *Cloud organisation on 6 November 1978*

The picture printout corresponding to 6 November (Fig. 3) gives the digital display of the cloud top temperatures over the cyclone area. Six different classes of temperature ranges have been contoured. Convective clouds are seen to occupy more area in the northern sector than in any other sector. The deepest convective cell with temperatures less than 219 deg. K is also located to the north. Just south of it a cell with temperatures 219-224 deg. K is seen surrounded by temperatures 224 deg. to 234 deg. K. There is also a small deepest cell near the centre. The pockets of subsidence are those with temperatures more than 272 deg. K, which are located about 300-400 km from the storm centre.

6.2. *Cloud organisation on 9 November 1978*

The picture printout of 9 November 1978 (Fig. 6), uncorrected for computer character distortion, can be seen to agree well with the satellite imagery. The spiral structure of the cyclone, the outflow blowing out of the centre and the eye of the storm are clearly discernible in the picture printout. There are 3 pockets of highest convective cell with temperatures less than 220 deg. K just north of the centre. Two small deep convective cells are surrounded by warmer clouds having temperatures 228-238 deg. K. The activity is seen to have concentrated more on the northern side.

One of the interesting features observed is the large areas of subsidence on the eastern side occurring beyond 300 km from the storm centre. The western side subsidence though not prominently seen in the picture printout is apparent from the distorted original imagery. The spiral bands separated by clear areas are very well seen on the eastern side.

Fig. 7 shows the temperature structure of the eye. The warmest temperature seen through the eye is a small cell of 295 deg. K temperature (without atmospheric corrections). The cloud wall is seen with temperatures less than 250 deg. K. The deep convective clouds are also noticed with temperature range 220-240 deg. K on both sides of the eye at a distance of about 20 km.

The cyclone, as a warm core system can be but only feebly inferred from the higher temperatures within the eye, compared to the surrounding, where the SST (uncorrected for atmospheric corrections) has been inferred to be about 290 deg. K. The temperature at surface within the eye are thus about 3 deg. to 5 deg. K more than those found adjoining the cyclone.

The fine structure details of the eye in relation to environmental temperature needs more detailed examination. The warm core would be more conspicuously observed at 200-300 mb level, where the temperature excesses are expected to be 10-12 deg. C from the surrounding (Kidder

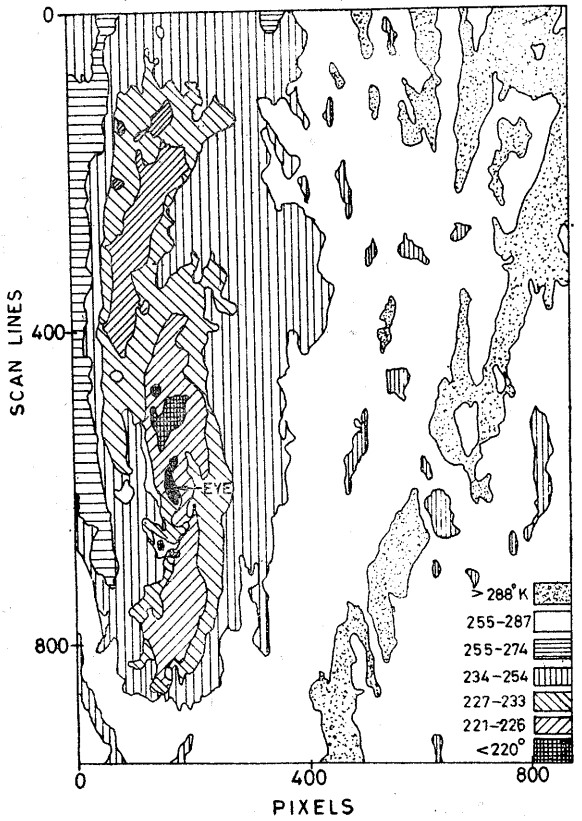

Fig. 6. Cloud top temperature map of 9 November 1978

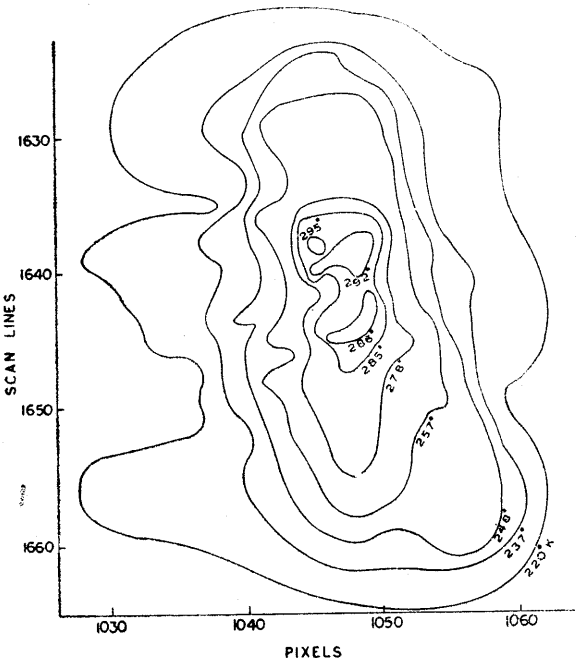

Fig. 7. Structure of the cyclone eye of 9 November 1978

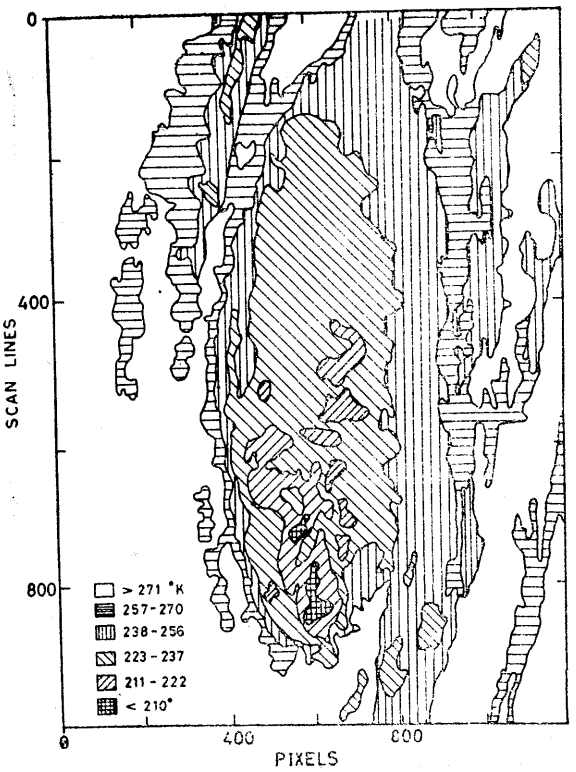

Fig. 8. Cloud top temperature map of 10 November 1978

TABLE 2

Date (Nov 1978)	Extra-polated T No.	Signifi-cant temp. range (°K)	Total cloud area defined by 255 °K contour (10^4 sq. km) (100%)	Mean T_B of total cloud area (°K)	Area of deep convective cells defined by 235°K: 10^4 sq. km	Area of deep convective cells defined by 235°K: % of total area	Mean T_B of convective area (°K)	Area of highest convective cell: 10^4 sq. km.	Area of highest convective cell: % of total area	Mean T_B of highest cell (°K)
06	4.0	216-290	67	236	36	54	229	6.2	9	219
09	5.5	212-292	57	236	30	53	228	3.2	5.6	215
10	4.5	200-290	48	234	28	58	225	1.2	2.6	205
11*	3.5	209-290	—	—	—	—	—	0.2	—	211
12**	—	270-290	—	—	—	—		—	—	—

*Only two bright patches of deep convection were analysed as cyclone had disorganised on 11th. Hence results for some of the columns do not exist.

**Lowest temperature is 270 °K, hence for other columns data do not exist.

et al. 1978). Observations of the warm core at these levels are planned using the TIROS-N Microwave Sounding Unit (MSU) data.

Fig. 7 reveals clearly the east-west asymmetric nature of the eye. Whereas on the western side the 220 deg. K contour is on the average about 15 pixels (equivalent to about 25 km) from the clear eye, the same on the eastern side is only about 12 pixels (about 15 km) from the clear eye area. The eye is, however, more symmetrical in the north-south direction.

6.3. *Cloud organisation on 10 November 1978*

The picture printout of 10th (Fig. 8) emphasises its importance in evaluating the strength of the cyclone. Although cirrus canopy in the satellite imagery appears as a uniformly bright disc, the picture printout allows one to easily identify various levels consisting of convective clouds. The spiral structure observed on 9 November is absent on this day.

The highest convective cell with a temperature range 200-210 deg. K is located in the southern sector of the bright CDO. It is embedded in another cell with temperature range 211-222 deg. K which is also situated more towards the southern sector. The northern portion of the CDO consists of relatively warmer clouds with temperature range 238-256 deg. K. It is interesting to note that though the cyclone had weakened on this day (as per T-No.) compared to 9th, the deepest convection on this day had reached nearly 2 km higher. The areas of subsidence denoted by temperatures in excess of 271 deg. K are located within about 100 km of the areas of deep convection.

6.4. *Cloud organisation on 11 and 12 November 1978*

On the morning of 11 November the cyclone had become completely disorganised. However, two bright patches of deep convective clouds are seen from the imagery. The lowest temperatures encountered were 210 deg. K. The areas of subsidence are also seen close ($\sim$50 km) to the areas of deep convection.

The imagery of 12 November (Fig. 4e) presents the cyclone after landfall. Even from the imagery it is clearly seen that higher level clouds are absent. The lowest temperatures encountered were only 270 deg. K indicating a sharp decrease in the cloud top heights in one day.

7. Discussions

Table 2 summarises the results presented in Sec. 6. For each day of observation, the area occupied by the 255 deg. K contour (defining the CDO cloud boundary), mean temperature within this contour, the areas occupied by the 235 deg. K contour (defining the deep convective region) and their mean temperatures are listed. The area and the mean temperature of the deepest convective cell are also included, besides the T-No. of the cyclone from Table 1 extrapolated to the time of satellite observation.

One striking factor noticed is the decrease in mean temperature of the deepest convective cell from 6th till 10th and an abrupt increase in the cloud top temperature associated with cyclone land fall on 12th. The cloud area defined by the 255 deg. K (CDO area) can be found to be decreasing from 6th through 11th.

The T-No. criteria of intensity estimate of the storm (Dvorak 1975) takes into account the size of the CDO (defined by 255 deg. K contour in our case) and the degree to which spiralling bands encircle the storm centre, besides shape of CDO, locating the eye etc.

It has been shown by several workers (*e.g.*, Arnold 1977) that no technique for relating storm intensity solely on cloudiness amount (CDO in our case) can specify storm intensity at individual time period. This is also supported by our observations of 255 deg. K contour area on the first three days when the cyclone was intense and organised.

Though T-No. for the 9th was the maximum amongst the days considered, neither the deepest convective cell temperatures, nor the CDO area of that day go to support this higher value in comparison to the other days of observation. One further interesting feature to note is that a comparison of the areas occupied by the highest convective clouds of 6th, (temperatures less than 219 deg. K) as a normalising factor indicates that on 10th, this area was nearly 75 per cent more than that for the 9th and almost equal to that of 6th. Though on 10th, the storm intensity had reduced from 9th (according to T-No.) the convection had gone to a greater height (by about 2 km).

This is in contrast to the observations of Shenk and Rodgers (1978) who report a 2 km drop in the maximum cloud top height associated with the decrease in hurricane *Camille* intensity. The present observations also do not support fully Gentry *et al.* (1978) hypothesis, particularly the last.

The present observations are partly explainable, however, by taking into account the location of the deep convective cells within the CDO and the separation distance of subsidence areas from the locations of deep convection on the different days.

Several investigations have observed a general tendency in the early stages of tropical storm formation or a concentration of deep convection near the incipient storm centre (Yanai 1968 ; Balogun 1973; Dvorak 1975). Yanai observed that in a developing cluster the precipitation area or general area of cloudiness approaches surface circulation centre as the cyclone intensifies. Dvorak (1975) noted that as the cyclone intensifies, the comma configuration is usually observed to become more circular with its central core clouds increasing in amount and density. Most investigations concerning the concentration of convection during early storm development have been case studies and there is little documentation in statistical sense to show a general tendency among developing clusters to concentrate their convection (Arnold 1977). Neither have there been any satisfactory explanations given for the physical processes attending such convective cloud concentration. Balogun (1973) used a form of vorticity equation to qualitatively relate the concentration of convection to the dynamics of the incipient cyclone, which, however, could not explain subsequent changes in convection beyond the depression stage.

An examination of the highest three convective cells in Figs. 4, 6 and 8 reveals a progressively southward location of these cells in relation to the cloud boundary (or CDO). On 6th when the cyclone was still intensifying the highest two cells were in the northern sector of the CDO with a small contribution near the centre. The next lower cell was more uniformly distributed with respect to the cloud boundary.

On 9th a larger portion of the highest convective cell is observed to the north of the eye, with two comparatively smaller cells south of it. The next lower convective cell, though more on the northern side, is to a large extent distributed equally on the northern and southern sectors. Most of the deep convection is still concentrated on the northern side.

On 10th, however, a drastic change appears to have taken place, with the highest convective cell (in this case having gone to a further height of 2 km compared to 9th) moving close to the southern edge of the cloud boundary. The next lower cell is also concentrated more to the southern sector, with the third lower cell more uniformly distributed.

An examination of the distance of the areas of subsidence from areas of deep convection reveals that they were more uniformly distributed around the storm at distances of 300-500 km on 6th. On 9th the distance of nearest areas of subsidence reduced to about 250-300 km. On 10th, however, the nearest areas of subsidence are located within about 100 km from the deepest convection cells.

The preceding arguments suggest that the deep convective cells on 10th had lost their close identity with the storm system and do not contribute effectively to the cyclone intensity changes. It may be surmised that if they had continued to be an inherent part of the system, then height drop of these convective cells would have been evident, when the cyclone intensity reduced, as was observed by Shenk and Rodgers.

Our observations pose new questions about:

(*i*) the southward shift of the deep convective cells in the CDO, more significantly noticed on the 10th, and

(*ii*) their higher convection associated with their southward location.

The points to be noted are the northeastward movement of the cyclone from 8 November and that on the 10th the northern part of the cyclone was lying over the land with the highest two deep convective cells lying over sea.

The upper air circulation for the above days indicate that the westerlies were moving southward, and on the 10th cyclone itself got embedded in the westerlies resulting in the weakening of the storm (Rao *et al.* 1980). The marked southward shift of the deep convective cells on 10th from 9th could be a likely result of the southward extension of the westerlies.

The progressively decreasing area occupied by the highest convective clouds (without regard to their temperature) on the different days of observations suggest that — the larger these areas, the more indications are that the storm will be intensifying further, intermediate values indicating almost a mature stage and low values suggesting a decay of the storm. A threshold area for these categories for the different phases of the storm, however, will need more detailed examination of a number of storms.

The aspects of location and distribution of deep convection in the cyclone area during its entire life-cycle and also at times of recurvature needs more detailed study. This is borne out from the results of 10th, where, although the 235 deg. K contour occupied nearly 95% of area compared to 9th and had deeper convection, still the storm had weakened. The reasons for this deeper convection despite weakening of the storm (as observed on 10th) also needs examination from more case studies.

8. Conclusions

Cloud top temperature maps from satellite data contain useful information regarding the intensity changes associated with the cyclonic storm. Analysis of the data during the life cycle of Saurashtra cyclone (1978) indicates the importance of the locations and distribution of the deep convective cells within the cyclone area. A progressive shift of the deep convective zones from the northern sector to the edge of the southern sector was observed as the cyclone intensified and finally decayed. The decay of the storm is explained as due to the shift of the convective cells to one edge and their getting away from the main system despite higher convection. The southward shift of the cells themselves are possibly due to the southward extension of the westerlies, which were explained as the cause of the weakening of the storm.

Acknowledgements

The authors are grateful to Dr. T.A. Hariharan, Head, Meteorology Division for his keen interest, constant encouragement and valuable suggestions during the course of this work. Useful suggestions from Prof. P. R. Pisharoty and Dr. D. R. Sikka are also sincerely acknowledged.

Grateful thanks are due to Mr. V. D. Thakkar for his valuable help in the processing of the data. Thanks are due to Dr. P. S. Desai for critically going through the manuscript and also other members of the Met. Division for useful suggestions and discussions. The recording and digitisation of the VHRR data has been done with the cooperation of the members of the Image Processing and Analysis Division and of the Communications Area of SAC.

References

Arnold, C.P., 1977, Tropical cyclone cloud and intensity relationships, Atmos. Sci. Paper No. **277**, Colarado State University, 154 pp.

Balogun, E.E., 1973, A study of satellite-observed cloud patterns of tropical cyclones, Project No. 108, Dept. of Geophysical Sciences, Univ. of Chicago, 103 pp.

Bhaskara Rao, N. S. and Saxena, V. P., 1977, Derivation of cloud top heights using HRIR data, *Indian J. Met. Hydrol. Geophys.*, **28**, 4, p. 447.

Dvorak, V. F., 1975, Tropical intensity analysis and forecasting from satellite imagery, *Mon. Weath. Rev.*, **103**, 420.

Dunn, G.E. and Miller, B. I., 1960, '*Atlantic Hurricanes*', Louisiana State Univ. Press, 123 pp.

Dvorak, V.F. and Wright, S., 1978, Tropical cyclone intensity analysis using enhanced infrared satellite data, Proc. 11th Tech. Conf. on Hurricane and Tropical Meteorology, 268 pp.

Erickson, C. O., 1979, Objective use of satellite data to forecast changes in intensity of tropical disturbances, NOAA—TM NESS, 103, 41 pp.

Follansbee, W. A., 1976, Estimation of daily precipitation over China and the USSR using Satellite imagery, NOAA TM **81**, 30 pp.

Garde, V. K. and Narayanan, M. S., 1978, Calibration procedure for the NOAA VHRR data, Technical Note RSA MET/T/11.1/2/78.

Gentry, R.C., Rodgers, E., Steranka, J. and Shenk, W.E., 1978, Predicting Tropical cyclone intensity using satellite measured equivalent blackbody temperatures of the cloud tops, NASA TM 79645, 34 pp.

Griffith, C.G., Woodley, W. L., Grube, P.G., Martin, D.W., Scout, J. and Sikdar, D. N., 1978, Rainfall estimation from geosynchronous satellite imagery—Visible and infrared studies, *Mon. Weath. Rev.*, **106**, 1153.

Kidder, S.Q., Gray, W. G. and Vonder Harr, T. H., 1978, Estimating Tropical cyclone central pressure and outer winds from satellite microwave data, *Mon. Weath. Rev.*, **106**, 1458.

Rao, B. M. Narayanan, M. S. and Sharma, A.V.S.R.K., 1980, A preliminary study of the Saurashtra cyclone from NOAA-5 VHRR imageries, *Mausam*, **31**, 2, pp. 225-228.

Rosenthal, S.L., 1978, Numerical simulation of tropical cyclone development with latent heat release by the resolvable scales, I-Model description and preliminary results, *J. atmos. Sci.*, **35**, 258.

Scofeld, R. A. and Oliver, V. J., 1977, A scheme for estimating convective rainfall from satellite imagery, NOAA TM NESS 86, 41 pp.

Shenk, W. E. and Rodgers, E. B., 1978, Nimbus 3/ATS-3 Observations of the evolution of Hurricane Camille, *J. Appl. Met.*, **17**, 458.

Thakkar, V. D., Rao, B.M. and Narayanan, M. S., 1979, Calibration of NOAA VHRR data-Part II-Results, Technical Note RSA/MET/11.1/1/79.